

Modeling of friction-stir butt-welds and its application in automotive bumper impact performance

Part 2. Impact modeling and bumper crash performance[†]

Sachin Patil^{1,*}, Yi Yang Tay¹, Farzad Baratzadeh^{1,2} and Hamid Lankarani¹

¹Wichita State University, Wichita, KS, USA

²Advanced Joining and Processing Laboratory, National Institute for Aviation Research, Wichita, KS, USA

(Manuscript Received July 23, 2016; Revised March 28, 2017; Accepted March 28, 2017)

Abstract

Ever increasing requirements regarding vehicle safety have led to rapid developments in various joining process. Among FSW widely used for Aluminum alloy welded structure of car body because of their remarkable performance in welding. For a better understanding of this performance, it is necessary to determine the behavior of butt weld in service conditions. In earlier phase of this study, thermo-mechanical simulations and analysis are performed to understand the thermal behavior in the FSW weld zones. The developed models are correlated against published experimental results in terms of temperature profile of the weld zone. The objectives of the second part of this work is to develop and demonstrate an FE model of bumper and crash box assembly that would improve on the current modeling techniques for the mechanical response of welds in structural problems.

Keywords: Friction stir butt welding (FSW); Thermal modeling; Johnson-cook failure model; Sled test; Vehicle bumper assembly

1. Introduction

With major development in the aluminum alloys, FSW welding now successfully used in the automotive industry. A fully coupled thermo-mechanical model of AA6063-T6 and AA6082-T6 for FSW was developed to examine the thermal history during the welding process. Detailed microstructure and property information in the weld region to properly formulate the constitutive equation applied using JC parameters. The next phase in this study is to predict the behavior of the bumper crash box assembly in crash events. This will then give necessary mechanical properties to use in crashworthiness problem rather than pure thermal properties one. The influence of thermal properties was investigated in this phase by modeling of FSW weld region using micro-hardness testing and material model development. A significant part of this section has been put into getting knowledge of the challenges that are valid for simulation results from phase one as well as experimental test on vehicle bumper part [1].

2. Impact modeling of FSW weld region

2.1 Micro-hardness testing

The modeling approach for the FSW weld model and the derivation of its material properties has been accomplished by micro-hardness test. The joint configuration investigated is a FSW butt welded joint having a wall thickness of 4 mm. A deeper understanding of the interaction between microstructures and solidification-induced defects in the weld region during the welding process of AA6063-T6 and AA6082-T6 is enabled by the use of micro-hardness testing and later numerical simulation. To characterize the individual material phases in FSW, it is not possible to directly measure the strength properties of the weld and HAZ material, therefore hardness is measured instead.

As shown in Fig. 1, the specimens of the hardness test are cut from the region of the weld and HAZ of welded specimen. The micro hardness test is performed on different rows of the specimens through the thickness after polishing the specimen. Vickers hardness is measured using a load of 5 kg along the centerline of the cross-section with 1mm distance between the measuring points [2]. A micro hardness profile interprets the microstructure of the weld and its mechanical properties in the vicinity of the weld affected zone in the FSW specimens.

Upper and lower surfaces of the weld measured different hardness values indicating the hardness for AA6063-T6 parent material higher than AA6082-T6. The hardness varied be-

*Corresponding author. Tel.: +1 316 2001716

E-mail address: sapatil1@wichita.edu

[†]Recommended by Editor Chongdu Cho

© KSME & Springer 2017

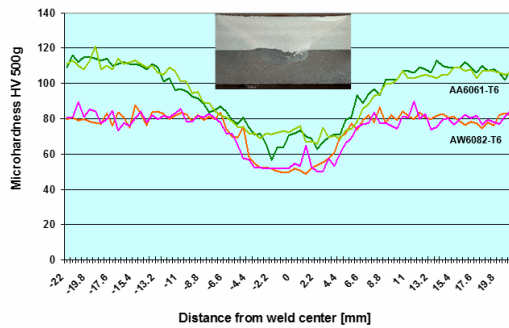


Fig. 1. Micro-hardness profile of the FS welded specimen [3].

tween 122 and 58 H_v for the top and 88 and 46 H_v for the bottom sheet, respectively. The parent material hardness is 118 H_v for the top sheet (AW6082-T6) and 80 H_v for the bottom sheet (AA6063-T6). The hardness has a minimum value of 60 H_v in a narrow region of the HAZ when compared to base material hardness 80 H_v . The micro-hardness result indicated that hardness values drastically decreases in the weld (nugget) zone and the average of the hardness is significantly lower than the parent material. This is due to the variation of the microstructures between the weld zone and parent material as well as different grain size of these two regions. Micro hardness tests characterize the Vickers hardness profile shows clearly a hardness decrease in the thermo mechanically affected zone and that the nugget zone average hardness is significantly lower than the base alloy hardness. Material flow, mixing of the two alloys, and the absence of the hooking is clearly identified in the micro structural analysis of the dissimilar lap joint. A detailed description of various zones characteristics can be found in Ref. [3].

The microstructure of the HAZ depends on the peak temperature attained and the length of time spent in the temperature range 500 to 380 °C. In particular, the grain size affects the stress-strain relations and a possible transformation behavior which the structure composition and thus in turn affects the stress-strain relationship. The material properties such as the yield strength and ultimate strength required for modeling of the stress field are estimated from the hardness data using an inverse engineering approach. This predicts the anisotropic flow stress and plastic flow in various region based on plastic strain evolution. Based on the hardness profile, different property assigned to the TMAZ and HAZ. Dissolution and growth of the precipitate in stir zone would result in a reduction of hardness and thus yield stress scaled down of the base metal [4]. Due to higher hardness observed in the TMAZ, yield stress increase of 1.2 from base metal was scaled. These values were based on the theoretical relations of hardness observed in each joint region for comparable grade of aluminum [5]. The benchmark case presented here confirms that material properties measurement using hardness data are suitable to generate input data for impact analyses, taking into account peculiar characteristics of yield stress variation, plastic dilatation and damage.

2.2 Weld modeling

Bumpers are welded using the GMAW and plunge FSW process and FSW vs GMAW fabricated bumper compared in a previous study [1]. In this study, new FSW welded beam-to-crash box joints are evaluated with referenced to old FSW modeling referred. The material card used to define the weld joint was MAT100_SPOTWELD in Ls-Dyna [6]. This is not consistent with the mechanics of the physical world, as there should be a significant deformation during impact test. This inconsistency is studied in detail by Patil et al. [7]. Efforts have been made in developing better models to resolve the inconsistency and to include wider range of experimental factors [7, 8]. Shell elements are utilised to discretize the FSW welded beam-to-crash box joints. In the macrostructure profile some important weld joint regions, including the nugget, TMAZ and HAZ, are identified for the models developed and the weld failure was shown to mimic the progressive tearing failure as desired [7].

In the current study, AA 6063-T6 is used to fabricate the bumper and AW-6082-T6 for the crash-box. The material properties is created based on results obtained from coupon testing and simulation is also verified using thermal history evolution of welding process as studied in phase 1. Values from the static tests reported using standard specimen coupon test are used to provide data for the failure stresses and strain data for use in material model. These detailed microstructure gradient data are then used in the stress calculations. The predicted micro-hardness results are then converted to the yield strength and used in the weld formulation. The Johnson-Cook shear failure model is suitable for high-strain-rate deformation of metals; therefore, it is most applicable to true dynamic situations. For quasi-static problems that require element removal, strain softening or the Gurson metal plasticity model is recommended [9]. A more detailed description of the Johnson-Cook failure model can be found in the Ls-Dyna user's manual [10] and Refs. [11, 12]. Compared with base material, friction stir welding process leads to a decrease in the material mechanical properties. Material properties of the weld, HAZ and base material are identified according to material tests and available experimental data. In order to accomplish this variation, a material model that accounts for complex material behavior must be formulated. The material characterization of ductile aluminum alloy is studied [13]. The material undergoes isotropic elasto-plastic behavior which can be reproduced by a Johnson-Cook model with damage. The cumulative effect the weld region properties variations is taken into the Johnson-Cook coefficients. Johnson-Cook coefficients adjusted to follow stress-strain curve in the weld region. Thereby increase the intensity of stress will simulate physically the contribution of each element in weld region. The element length in the model of the bumper is about 4 mm as used whereas in weld region element size is same (0.8 mm) as in the FE model of the tension test on a smooth flat specimen. These are simulated for the determination of the Johnson-

Cook parameters [14, 15].

Regarding the FE model for welded structures, shell elements are mostly used to capture the structural behavior efficiently. Depending on the choice of the element order, mesh size, etc., local nominal or even hot spot stresses can be calculated. The shell properties are 5 integration points, Belytschko elasto-plastic hourglass formulation (Ishell = 3), iterative plasticity for plane stress, thickness changes are all taken into account in stress computation. The initial weld thickness is uniform, equal to 4.0 mm. The Ls-Dyna is utilized for the finite element analysis in plastic-dynamic problems with material failure defined. This validates thermo-mechanical model of FSW as discussed. Also Lap shear test were conducted to determine mechanical properties of welded specimens [3].

2.3 Weld contact modeling

Dynamic problems involving contact are of great importance in industry related to mechanical performance. Further contact formulations are defined between weld and structure (nodes to surface). A tied contact is defined to fix the weld nests to the inner bumper panel and crash box. Nevertheless, a force transducer contact formulation has been applied to determine the contact forces between each weld nest and outer crash box, representing the load response of FSW. For the contact problem, only reduction in the contact thickness limited to this weld area need to be mastered. i.e. adjusting contact thickness to illustrate failure. Shell elements with reduced integration points help a relevant degree of calibration to obtain good contact interface. The weld are usually modeled using the CONSTRAINED_SPOTWELD keyword. In this keyword spot welds are defined as rigid beams that connect the nodal points of pairs of nodes, coupling nodal rotations and displacements. Brittle and ductile failure can be specified through the introduction of normal and shear limit forces or effective plastic strain at failure, respectively [16, 17]. Contact condition help to model process forces during joining which give insight to residual forces. Tied contact is a connection between the weld and bumper crash box have been implemented. Constraint based contact showed that a number of welds failed due to force build up in the welds region as per SIGY and ETAN values used in the materials model. Failure of the contact interface is defined in LS-DYNA by the inclusion of normal and shear failure stresses. In this area, the contact thickness is corrected as:

$$\left(\frac{\sigma_n}{A_{fail_N}}\right)^{A1} + \left(\frac{\sigma_s}{A_{fail_S}}\right)^{A2} \leq 1 \quad (1)$$

where n is the stress normal to the interface; s is the stress in shear directions; A_{failN} and A_{failS} are the strength coefficients, A1 and A2 are constant/exponent. In this method, the contact stiffness remains constant but the overlap can be thought of as being scaled over a certain interval.

2.4 Bumper-crash box joint configuration setup

In order to evaluate the strength of the welded assemblies in a dynamic condition, traditional sled testing for low speed bumper requirements are performed. In the full frontal low speed test procedure, the car impacts a rigid wall at 20 kph (12.4 mph) [18]. This procedure is used by the National Highway Traffic Safety Administration (NHTSA) for full width frontal impact collisions.

The vehicle used in the full-scale tests is known as carriage. It is a reusable unpowered four-wheeled structure with a frontal deformable nose. By varying the arrangements of the honeycomb cartridges and number of dead weight plates, the carriage can be calibrated to replicate the behavior of an actual vehicle using Part Inertia to avoid pitching. The crash-box is an attachment element for a bumper that includes a partially closed profile with a back panel wherein this attachment element is fusion welded, traditionally, as a part of the bumper. The model is constructed using 4 node quadrilateral shell elements to represent the sheet metal (2356 nodes and 2200 shell elements). This attachment element acts as crash absorbing element which can absorb shock impacts of up to 4 km/h in an elastic range and at shock impacts between 4 km/h and 20 km/h, the crash absorbing elements deform thereby preventing damage to the vehicle carrier.

In this section, a bumper and two crash-boxes configurations are assembled to replicate slow speed crash behavior at 15 and 20 kph. A validated finite element model of LSTC carriage is developed to simulate the low speed full-scale crash tests and has been published in Ref. [20]. This simulation is analyzed and validated for its bumper impact test. The sled tests were conducted in April and May 2010 using the dynamic driving simulator sled test at National Institute for Aviation Research and Innovation Center / WSU. Special aluminum rod or wire used to arc weld usually GMAW welding. The FSW of the bumper to the crash-box is carried out on a five axis MTS I-Stir Process development system (PDS) at the NIAR. All the components are welded in the "T6" condition. The GMAW of the bumpers and crash-boxes were fabricated at the welding lab located at National Center for Aviation Training (NCAT). Details of the model developments and validations are described in Ref. [18]. The main objective of this setup was to study the effects of low speed impact on bumper and the potential weld failure to understand the GM bumper deformation at various impact conditions [19].

Fig. 2 shows configuration for the sled simulation and experimental setup, as well as mesh details in the weld zone. The carriage center of gravity accelerations and the wall forces were plotted versus time and post-deformation compared. The deformation predicted using new FSW Johnson cook model (MAT_15) weld found closer to the experimental test than the one predicted [20]. Following simulation results confirms this in detail.

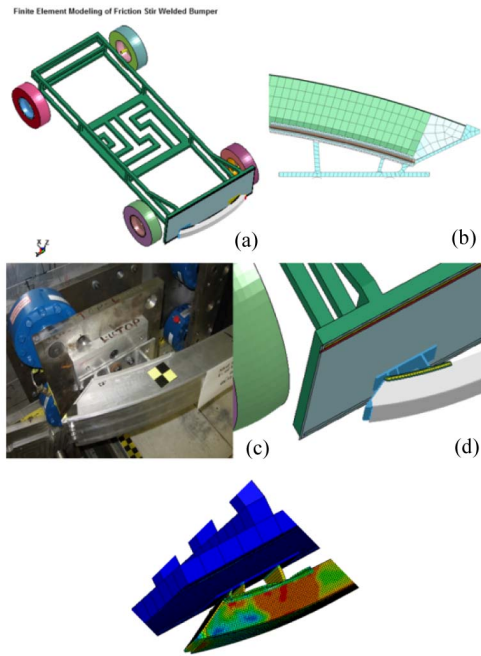


Fig. 2. (a) The full-frontal sled simulation setup; (b) finite element mesh of the bumper/weld joint assembly; (c) sled test configuration [20]; (d) numerical modeling for the weld joints.

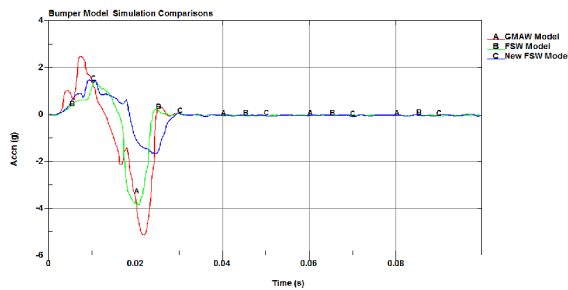


Fig. 3. Barrier acceleration for the 20 kmph full-frontal test.

3. Result and discussion

3.1 Comparisons of acceleration pulses

The acceleration time histories are recorded at the center of gravity of the carriage. Acceleration pulses are filtered using a SAE 60 Hz filter. The mass of the plates and the box in the model corresponded to those of the actual accelerometer assembly used in the test. There are four three different parameters which affects the acceleration, the speed of the vehicle, weight of the vehicle, area of the impact and weld quality. By keeping the first three parameters constant, the quality of the weld when subjected to impact can be evaluated. It was found that the FSW on aluminum bumper help enhancing the crash performance in term of energy absorption as discussed further.

New FSW weld methodology reduce the number of load path, soften the front end which allowed greater crush of frame. This better energy absorption capability increases impact duration and produce lower overall g value. Old FSW model shows stiffer response due no weld failure which does

Table 1. Acceleration pulse comparison for the 20 km/hr full-frontal test (Exp and sim results).

		Avg G	% Δ	Peak G
Experimental results		3.03	-	5.1
FE results	Old FSW fabricated bumper	2.83	2.6 %	3.8
	New FSW fabricated bumper	2.78	3.1 %	3.9

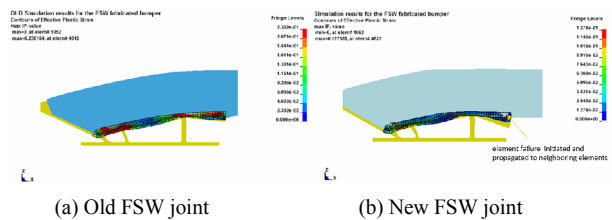


Fig. 4. Plastic strain comparison for the old and new FSW bumper/crash-box assembly.

not correlates well with the test carried out. Acceleration pulse is shown to be less severe in the new FSW weld model due to better representation of weld failure illustrated in Fig. 3. When deceleration pulse drop by 3 g, the collapse load is found to be increased by 11 %. Acceleration pulse is quite sensitive to corresponding material properties defined in weld. In the old FSW weld model, early bending of crash box region instead of linear crush dictates higher peak during crash event. The greatest magnitude of the acceleration was about 3.8 g’s for the FSW bumpers where the magnitude of the carriage CG acceleration was 5.1 g’s for the GMAW bumper. This can be another reason that indicates that FSW fabricated components increases the amount of energy absorption when compared to GMAW fabricated components. As shown in Table 1, the acceleration of the new FSW fabricated bumper is lower than the old FSW fabricated bumper. The peak load in the present beam is around 2.7 g’s whereas in the old FSW weld the CG’s acceleration is around 2.8 g’s. It can be seen that the acceleration decreases by 3 %.

3.2 Post-crash comparison

The strain distributions and Von Mises stress of the corresponding weld models are discussed in this section. Current model shows better result in term of lower strain and lower deformation. For better visualization of the deformation near the weld area, the exaggerated view of the left side bumper and crash-box assembly for both the old and new FSW fabricated bumpers are shown in Fig. 4.

The new FSW weld shows less local strain (0.12). Relatively larger tensile stress is required to further increase plastic strain in the soft core in FSW welding. Thus effective stress is higher in weld region when compared to base material. As a result lesser strain found in new weld model resulting less deformation and more strength of weld. Element deletion

Table 2. Comparison of Von-Mises stress (VMS) for the 15 and 20 kph impact.

Impact speed	Von-Mises for old FSW fabricated bumper (MPa)	Von-Mises for new FSW fabricated bumper (MPa)	Reduction (%)
15 kph	303	273	9.9
20 kph	314	297	5.4

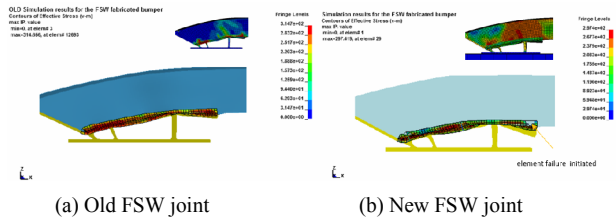


Fig. 5. Von-Mises stress comparison for the old and new FSW bumper/crash-box assembly.

were observed at the impact duration which capture deformation well with the test. The old FSW weld model observed to take more distortion due to higher local strain (0.23).

Microstructure evolution was not effective in GMAW when compared to FSW weld resulting into more deformation in weld zone and HAZ due to slightly too high strain region observed. Higher strains were expected as per increasing strain rate and elongation. Thus if the local strain is taken as the failure criteria, it can be clearly seen that the model with major in plane strain at failure based upon the local strain (0.12) is better and can be compared with the old FSW weld model (0.23). When the local strain reaches the limit strain, the element erosion is initiated as shown in Fig. 5, and they are propagated to neighboring elements.

The failure of the bumper and crash-box assembly is analyzed using von-Mises stress (VMS) to predict the failure or the yielding of the numerical model. For comparison purpose, the VMS of the bumper and crash-box assembly at 15 and 20 kph crash velocities is shown in Table 2. The stress values found are close to the yield stress of the weld zone structure, leading to deformation without failure due to soft core region observed in this low hardened zone. The stress levels increased significantly as the impact speed increased. The old FSW weld configuration VMS reaches 314 MPa. A lower stress values 297 MPa for new FSW weld configuration indicate that bumper beam can take more load altogether safe design. It would not have reached the plastic range since the VMS is much less than the yield strength of the material. The results were not significantly off percentage wise for both model comparisons. Therefore no more tuning was done.

The deformation sequences of the rigid wall impact on an bumper crash box assembly – test and simulation, depicted in Fig. 6 shows a good similarity to the structural response. The figure shows the evolution of damage zone through the thickness of the top face of weld at 20 kph speed. Only half of the damage zone is depicted owing to symmetry. It is found that

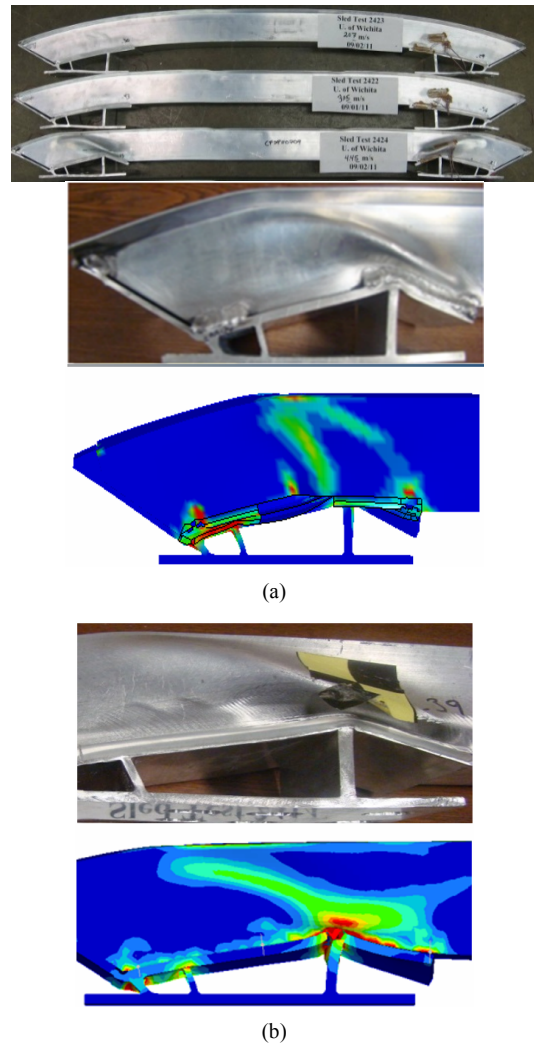


Fig. 6. Post-crash comparison study of the damage zone: (a) GMAW weld joints; (b) FSW weld joints.

damage was initiated in the weld zone. Further increase in speed led to growth along weld length. This result is found to be in a reasonable agreement with the measured one, as shown in Fig. 13. No complete separations or unstable crack growth in the FSW weld joint while weld separation for the GMAW method occurred at all test speeds as studied in Ref. [20]. New FSW joints were observed to bend over on themselves and did not exhibit visible rupture or cracking within the weld joint. After validating results with experimental data, it is also found that plastic strain in the new FSW is lesser compared to GMAW welding which indicates overall less deformation of bumper specimen. Force time history of the new FSW fabricated bumper are based on failure material model properties defined. The impact energy dissipated by frontal parts observed to be 93.8 % of the total energy (G1stat) and more strength of FSW can be anticipated from force vs time, as seen in Fig. 7.

To correlate this force time history with old CAE data, the recalibration process were iteratively performed to adjust the

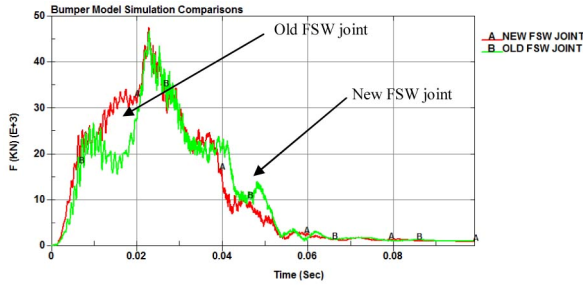


Fig. 7. The Force response of FSW bumper/crash-box assembly.

contact interfaces of the new FSW weld model. The recalibrated weld model is labeled new FSW model. As shown in Fig. 14, the load transfer in both weld model are comparable and force level is within the average corridor line of the Test load of 49.7 kN. The initial load ramping, the peak load and the rebound are accurately captured by the CAE simulation. Again, the initial part of the Force-time curves (till 0.02 sec of time) match line-on-line showing a very high level of correlation. A maximum force of 47.2 kN was noted in the simulation, which was about 3 kN greater than old FSW weld Joint model discussed in Ref. [20]. This difference might be attributed to greater frontal rigidity in the model. The force predicted by both FE models are in good agreement with the experimental response. Hence it can be predicted that new FSW weld are better to transfer residual forces from the bumper to the crash box. The variation of the stress-strain curve is not essential to study but rather the surface under the curve which characterizes the energy dissipated during the test. This energy-based approach is relevant for crash tests since the final assessment is often more significant than how it was achieved. As the area under the curve indicates the energy absorbed by the structure, it is evident from Fig. 14 that the structure with new FSW weld absorbs more energy. The new FSW weld as seen has a higher ability to withstand load 47.2 kN for 20 kph impact speed.

3.3 Deflection measurements

Data from the load cells on the test wall allow comparisons of displacement metrics as well between the crash test and simulation. Fig. 8 shows the total vehicle displacement, which tracks closely in both test and simulation over time, but particularly well up to 0.1 sec. This is considered important as displacement is a critical performance metric.

The old FSW weld (JC) model used previously overestimated the displacements. Overall the scatter between both weld models are small. The agreement is equally good for the simulation with the GMAW weld model (Table 3). A graphical comparison for bumper deflection in the full-frontal test using FSW and GMAW fabricated bumper is shown in Fig. 9. The penetration of the leading edge of the bumper with respect to attack face of the barrier is calculated.

It can be seen that displacement increases up to 0.023 sec

Table 3. Bumper deflection comparison of the experimental and simulation results for the two FSW variant bumper and GMAW fabricated bumper [1, 20].

Deflection comparison		Speed 20 kph	Speed 15 kph
Experimental results [20]	FSW	79.8	45.5
	GMAW	84.0	46
FE results	New FSW	74.6	43
	Old FSW [1, 20]	77.3	57

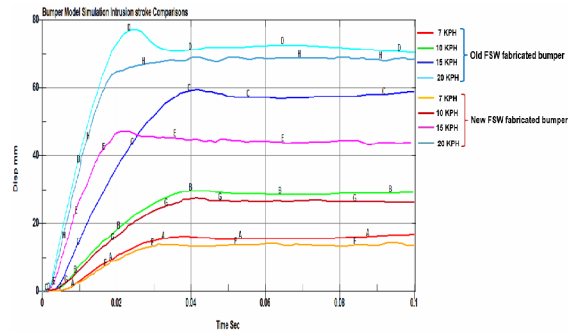


Fig. 8. Deflection comparison based on FE results of new FSW and old FSW at four different crash speeds.



Fig. 9. Bumper deflection measurement method [20].

since vehicle does not lose its kinetic energy. Furthermore it decreases after 0.040 sec due to vehicle spring backs from the barrier. Penetration limit does not exceed set target 87 mm as it can be seen in Fig. 8.

It is observed that as the crash speed increased, the rise time for the deflection curve increased due to the lesser time needed to deflect the bumper at higher crash speeds. With the exception of the 15 kph crash speed; the bumper deflections using new FSW Weld bumpers are generally lower than that of GMAW bumpers and old FSW bumpers. The deformation is more controlled now at the frontal part of bumper crash box weld region than later part, which reduces the displacement of the CG Barrier. Thus new weld modeling shows high amount of plastic deformation. Area under the displacement curve shows the amount of intrusion in the carriage. For the 15 kph crash speed, the results is not correlating well for old FSW bumper deflection data. The contributing factor to these correlation differs, especially for 15 kph crash speed, may be due to the inability to properly define the crack propagation of the weld joint.

3.4 Finite element validation

The overall crash response is composed of contributions

from the bumper, crash box and weld region. The carriage model was crashed into the walls at a speed of 15 and 20 kph. The new FSW model compared to old FSW model is attractive in that it significantly reduces strain and von-mises stress. These results show that the new FSW model can be used with reasonable accuracy for investigating weld performance. It is clear that the simulation captures the overall trend in a reasonable manner compared to the test. The impact event is simulated for a period of 0.1 s, and various quantities of interest are extracted from the finite element results including: Impact force versus time relationship, stress and strain values at key points. Similar studies by Baratzadeh et al. [20] conducted compared with this new FSW weld model. It is found that the present model takes 27 % more force than the old FSW model without failure of weld. The results in Fig. 8 indicates that the simulation correlate well with the test. It can be concluded from these comparisons that the model correctly predicted the behavior of the modified new FSW weld model in different speed tests. This adds fidelity and trust to the methodology used in developing the weld joint models. Further research is being conducted to analyze other parameters in the weld zone cracking system to investigate other impact scenarios. These parameters include the crack tip and location. The possibility of weld model as a result of variation of these parameters and influence of FSW welds on the folding mode and the crack initiation will be investigated in future.

4. Conclusions

The current paper is an investigation study of thermal history was conducted in phase one to understand FSW process and precedes the planned weld joint crash testing experiments to suit its practical application. Weld joints were characterized for mechanical properties from produced thermal properties of weld process. The most obvious desirable endeavor achieved is the correlation of the results of actual, physical experiments with the same material properties and geometry for the aluminum bumper beam under similar loading and restraint conditions against our models. This coupling between welding and crash simulation may be desirable to quickly transfer results from welding simulation to crash models. With this methodology, there is high potential to improve simulation based decision making and to reduce time required for finalizing a vehicle design. New material challenged with the test to deliver better correlation. The new weld decreases intrusion by 3.5 % with approximately 95 % of energy dissipated through deformation in the weld. Failure mechanisms in the tests and simulations were compared to ensure that the model provides a useful tool for exploring weld fractures and dislocations energy resulting from impact crashes. This is because FSW produces soft core region (more ductile nature in HAZ and WZ). The FSW weld initiates controlled smooth crush and further increases energy absorption. Although aluminum has less stiffness compared to steel. However after welding soft weld core absorb more energy for aluminum as material used.

In general good correlation with WSU NIAR-test results for crushing distance-time curves, which are the base all inputs for the discussed FSW setup in this study. Future works may include friction stir welding the bumper to a full-sized vehicle model to provide a more accurate analysis of the response of the vehicle in a more realistic frontal crash scenario.

Acknowledgement

Authors extend their special thanks to National Institute for Aviation Research (NIAR) for comparing the crash tests results of FSW and GMAW welding process in this research.

References

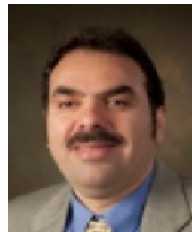
- [1] F. Baratzadeh, Friction stir weld development and dynamic crash testing of bumper crash box assemblies mad from dissimilar aluminum alloys extrusions (AA6082-T6 AND AA6063-T6), *Ph.D. Dissertation*, Wichita State Univ. (2013).
- [2] *Standard DIN EN ISO 6507 part 1 01.98*, Metallic materials - Hardness test Vickers - Test methods.
- [3] F. Baratzadeh, A. B. Handyside, E. Boldsaikhan, H. M. Lankarani, B. Carlson and D. Burford, Microstructural and mechanical properties of friction stir welding joints of 6082-T6 with 6063-T6, *Friction Stir Welding and Processing VI*, TMS (2011).
- [4] F. Zhili and S. Simunovic, *Impact modeling and characterization of spot welds, ORNL and Auto/Steel Partnership report*.
- [5] K. Dudzik and A. Charchalis, Influence of friction stir welding on hardness distribution in joints of AlZn5Mg1 alloy, *Solid State Phenomena*, 199 (2013) 430-435.
- [6] F. Seeger, M. Feucht, T. Frank, B. Keding and A. Haufe, An investigation on spot weld modelling for crash simulation with LS-DYNA, *4th LS-DYNA Forum*, Bamberg, Germany (2004).
- [7] S. A. Patil and H. M. Lankarani, Modeling and characterization of spot weld material configurations for vehicle crash analysis, *Proceedings of the 10th Annual GRASP Symposium*, Wichita State University, Apr. (2014) Wichita, KS, USA.
- [8] S. A. Patil, Modeling and characterization of spot weld for crash analysis, *Ph.D Dissertation*, Wichita State Univ. (2014).
- [9] F. Andrieux, D.-Z. Sun and H. Riedel, Development and application of a micromechanical model for the description of the growth and coalescence of spheroidal voids, *IFAMST 4th International Forum on Advanced Science and Technology*, Troyes, France, July 4-7 (2004).
- [10] *LS-DYNA Keyword User's Manual, Version 971*, Livermore Software Technology Corporation (LSTC) (2010).
- [11] A. Needleman and V. Tvergaard, *On the finite element analysis of localized plastic deformation*, Division of Engineering, Brown University (1982).

- [12] D.-Z. Sun, A. Höning, W. Böhme and W. Schmitt, Application of micromechanical models to the analysis of ductile fracture under dynamic loading, *National Symposium on Fracture Mechanics*, 25 (1995) 343-357.
- [13] P. A. Du Bois, S. Kolling and W. Fassnacht, Material modeling with LS-DYNA for crashworthiness analysis, *LS-DYNA Forum*, Bad Mergentheim, Germany, V2 (2002) 1-56.
- [14] B. Yingbin and W. Tomasz, A comparative study on various ductile crack formation criteria” impact and crashworthiness laboratory, *Journal of Engineering Materials and Technology*, 126 (3) (2004) 314-324, Doi: 10.1115/1.1755244.
- [15] G. R. Johnson and W. H. Cook, Fracture characteristics of three metals subjected to various strains, strain rates, temperatures and pressures, *Engineering Fracture Mechanics*, 21 (1985) 31-48.
- [16] D. S. Jeremy, A. Gilar, A. K. Jerome and R. L. John, High strain rate, high temperature constitutive and failure models for EOD impact scenarios, *2007 SEM Proceedings* (2007).
- [17] J. H. Song, H. Huh, H. G. Kim and S. H. Park, Evaluation of the finite element modeling of a spot welded region for crash analysis, *International Journal of Automotive Technology*, 7 (3) (2006) 329-336.
- [18] National Highway Traffic Safety Administration, <http://www.nhtsa.dot.gov> [cited 2014].
- [19] Crash Dynamics Laboratory, Research and Development Facility, *General Motors Cooperation*, Detroit, MI, USA.
- [20] F. Baratzadeh, Y. Tay, H. Lankarani and S. A. Patil, An experimental and numerical investigation into the dynamic crash testing of vehicle bumper fabricated using friction stir welding and gas metal arc welding, *International Journal of Crashworthiness*, Paper No. IJCR. 828.
- [21] T. Hasan, H. N. Tien, S.-H. Hur and Y.-J. Kwon, Mechanical properties of graphite/aluminum metal matrix composite joints by friction stir spot welding, *Journal of Mechanical Science and Technology*, 28 (2) (2014) 499-504.
- [22] S. Baragetti and G. D’Urso, Aluminum 6060-T6 friction stir welded butt joints: fatigue resistance with different tools and feed rates, *Journal of Mechanical Science and Technology*, 28 (3) (2014) 867-877.



Sachin Patil is doctoral student of Dr. Hamid Lankarani, Mechanical Engineering at Wichita State University. He has specialized in the application of explicit integration techniques for crashworthiness and impact weld failure problems. He has over 15 years of expertise in the field of numerical simulations,

and have the distinction of being qualified as crash analyst with weld failure propagation. He has authored scholarly articles in the crashworthiness, optimization field, in professional as well as major trade publications and consult on the use of numerical simulations using LS-DYNA/ABAQUS.



Hamid Lankarani is a Professor of Mechanical Engineering and a Senior Fellow of the National Institute for Aviation Research, at Wichita State University. He began his professional career in 1981. Dr. Lankarani is one of the world’s leading researchers and educators in the field of impact dynamics,

automotive and aircraft crashworthiness, occupant protection, and injury biomechanics.